Jurnal Aplikasi Teknik Sipil
Volume 24, Nomor 2, Mei 2026

Journal homepage: http://iptek.its.ac.id/index.php/jats

Comparative Seismic Performance Analysis of a 30-Story Building Structure with CFST Columns Using Concentrically Braced Frame and Moment Resisting Frame Systems

Yehezkiel Septian Yoganata[1,*], Kharisma Nur Cahyani[1], Kartika Purwitasari[1], Aulia Rahman[1], Sugeng Riyanto[1], Deni Putra Arystianto[1], Sri Heny Hidayati[1]
Civil Engineering Department, Politeknik Negeri Malang, Malang[1]
Koresponden*, Email: *yehezkielseptian@polinema.ac.id*

Info Artikel
Diajukan 16 September 2025
Diperbaiki 14 November 2025
Disetujui 22 Mei 2026

Keywords: steel building, CBF, MRF, CFST, lateral forces

Abstract

High-rise buildings in earthquake-prone areas often utilize Moment Resisting Frames (MRF) and Concentrically Braced Frames (CBF) for seismic resistance. While MRF is common for multi-story structures relying on beam-column connections for load transfer, the CBF system is generally superior for high-rise seismic applications. CBF uses concentrically placed bracing that resists lateral loads through axial action, ensuring efficient load distribution. This research focuses on the structural analysis of seismic loads by modeling a 30-story structure utilizing Concrete-Filled Steel Tube (CFST) columns, reinforced concrete slabs (f'c = 40 MPa), and Wide Flange (WF) beams. The building is designed to be located in the Indonesian Capital City (IKN). The results show that the maximum displacement for the CBF system is 98.496 mm and for the MRF system is 123.972 mm. The structural mass of the CBF system is 348,920.632 kN and the MRF system is 372,651.354 kN. Additionally, the maximum drift for the CBF system is 22.544 mm and for the MRF system is 30.791 mm. This confirms the CBF system's enhanced capability to withstand earthquake forces.

Kata kunci: bangunan baja, CBF, MRF, CFST, gaya lateral

Abstrak

Gedung bertingkat tinggi di daerah rawan gempa sering kali menggunakan sistem Rangka Momen Penahan (MRF) dan Rangka Pengaku Konsentris (CBF) untuk menahan gaya seismik. Meskipun MRF umum digunakan pada bangunan bertingkat yang mengandalkan sambungan balok-kolom untuk mentransfer beban, sistem CBF umumnya lebih unggul untuk aplikasi seismik pada gedung tinggi. CBF menggunakan pengaku yang ditempatkan secara konsentris yang menahan beban lateral melalui aksi aksial, memastikan distribusi beban yang efisien. Penelitian ini berfokus pada analisis struktur terhadap beban gempa dengan memodelkan struktur 30 lantai menggunakan kolom Baja Berisi Beton (CFST), pelat beton bertulang (40 MPa), dan balok Wide Flange (WF). Direncanakan gedung ini berlokasi di IKN. Hasilnya menunjukkan bahwa displacement maksimum pada sistem CBF 98.496 mm dan MRF 123.972 mm. Massa struktur pada sistem CBF 348,920.632 kN dan MRF 372,651.354 kN. Serta untuk drift maksimum pada sistem CBF 22.544 mm dan MRF 30.791 mm. Hal ini membenarkan peningkatan kemampuan sistem CBF dalam menahan gaya gempa.

1. Introduction

The relocation of Indonesia's new capital city (IKN) is a strategic step to support the vision of Indonesia 2045, which targets inclusive and equitable economic growth. This strategy aims to accelerate development in Eastern Indonesia while shifting the focus of development from being centered on Java Island to encompassing the entire nation.

In the context of high-rise building construction in the IKN area, there has been no comparative study to date between CBF and MRF systems for structures utilizing CFST columns. The implementation of the Concentrically Braced Frame (CBF) system with CFST columns is expected to be a solution for enhancing high-rise building earthquake resistance, utilizing the RSA Cipta Karya response spectrum parameters for IKN. The CBF system, which utilizes steel frames with diagonal bracing elements, is designed to withstand lateral forces generated by seismic activity. The main advantage of this system lies in its material efficiency and its ability to dissipate seismic energy effectively, thereby reducing the risk of structural damage [1]. The application of CBF systems is particularly relevant to support the development of multi-story buildings in IKN, which is categorized as having a moderate level of seismic risk.

Over the past few decades, advancements in construction technology and design methodology have continued to progress, including the application of bracing systems in tall buildings. The CBF system has become a popular choice due to its simplicity in both design and construction, as well as its

effectiveness in enhancing the lateral stiffness of buildings [2]. The concentrically braced frame system provides adequate stiffness through the use of bracing elements [3]. Steel frames reinforced with bracing offer excellent ductility and lateral stiffness, as the bracing elements integrate well into the system, ensuring that yielding occurs only in the bracing members without damaging the main structural elements [4].

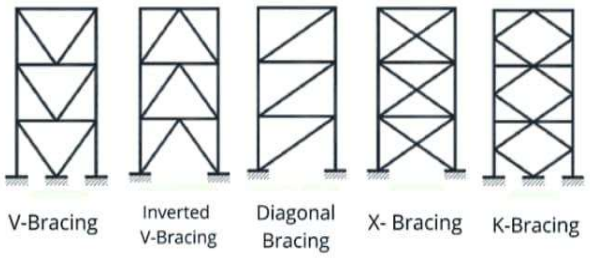

Figure 1. *Different types of bracings [5]*

Several bracing configuration forms in the CBF system are shown in ***Figure 1****. The different types of structural arrangements of bracing include V-Bracing, Inverted V-Bracing, Diagonal Bracing, X-Bracing, and K-Bracing. The configuration of concentric bracing significantly influences the structural behavior in resisting seismic forces, particularly in terms of stiffness, failure mechanisms, and energy dissipation [5] [6]. These effects need to be analyzed according to the actual structural behavior, as they indicate the level of structural resistance and the possible deformations depending on the bracing configuration employed [7].*

In recent years, the use of braced frame systems has been expanded to achieve both stiffness and ductility in structures located in high-seismicity regions. Several recent studies have discussed the effectiveness of concentric bracing in enhancing the stiffness and stability of tall building structures. The application of concentric bracing systems in high-rise buildings can significantly reduce lateral deformations; however, their performance strongly depends on the type of bracing configuration used [3] [8]. Furthermore, concentric bracing systems are capable of minimizing structural damage caused by seismic loads in tall buildings when the configuration is appropriately adjusted to the seismic conditions of the region [4]. The use of bracing also reduces displacement values, and from the perspective of serviceability, the CBF system is highly effective in resisting potential lateral forces [9]. The addition of concentric bracing to a steel frame increases its lateral stiffness, which in turn shortens its resonant period and generally reduces lateral storey drift. The bracing also minimizes bending stresses and shear forces in the columns, while simultaneously increasing the axial forces in the columns to which they are connected [10].

Concrete Filled Steel Tubular (CFST) structures are highly efficient because the steel tube and the infilled concrete work together to resist loads. CFST structures are widely used in the construction of skyscrapers and bridges [11]. From a behavioral perspective, CFST structures are not only superior in resisting static loads but also demonstrate excellent performance under cyclic loads, such as those induced by earthquakes or strong winds. This performance can be observed through three main aspects: favorable hysteresis curves, ductility, and high energy dissipation capacity [12].

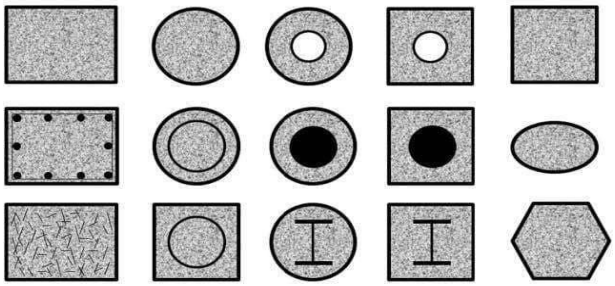

Figure 2. *Several types of CFST column cross-section [13]*

In addition, one of the characteristics of a CFST column cross-section is its ability to increase stiffness and strength. The steel tube confines the concrete within it (the confinement effect), which significantly increases the concrete's compressive strength and ductility. At the same time, the concrete prevents local buckling of the steel walls, thereby increasing the overall strength and stiffness of the column. This interaction allows CFST columns to have a much higher axial and lateral load capacity [14].

The steel tube serves as permanent formwork, eliminating the need for traditional formwork. This accelerates the construction process, saves on labor costs, and reduces completion time. Due to their high combination of strength and ductility, CFST columns have an exceptional energy absorption capacity. This makes them highly effective in resisting cyclic loads generated by earthquakes, making them an ideal choice for buildings in earthquake-prone areas [15].

With greater strength capacity, CFST columns can be designed with slimmer cross-sectional dimensions than conventional reinforced concrete columns for the same load. This is a significant advantage in high-rise buildings where space-saving is highly valuable. However, one of the main challenges in using CFST columns is the complexity of designing the connections between the columns and beams. These connections must be designed with extreme care to

ensure adequate strength, especially for resisting earthquake loads [16].

However, challenges arise when dealing with buildings of significant height, such as 30-story structures, where the increase in lateral forces is directly proportional to the building's height. Therefore, a thorough evaluation of the performance of concentric bracing in tall buildings is essential. It should be noted that the use of CBF systems in high-rise structures also has limitations. At certain heights, concentric bracing may lead to increased internal forces in other structural elements, such as columns and beams, potentially causing local failures if not properly designed [17]. Consequently, a more comprehensive assessment of the role of concentric bracing in tall buildings is required, taking into account parameters such as material properties, bracing configuration, and the seismic conditions of the construction site.

2. Research Method

The research stages begin with a literature review, followed by design planning. The design is based on two systems: the Concentrically Braced Frame (CBF) and the Moment Resisting Frame (MRF). A model of both systems is then created, followed by a structural analysis using the response spectrum method. Next, a control check is performed on the models to obtain results regarding the structural mass, base shear, displacement, and story drift. After that, the two models are compared by examining their effectiveness against earthquake forces. The building is planned to be located in IKN (Indonesia's New Capital city, Nusantara), and will function as an office building with 30 stories (floor-to-floor height of 4 m). The main structure employes steel as the primary material with structural systems of CBF and MRF.

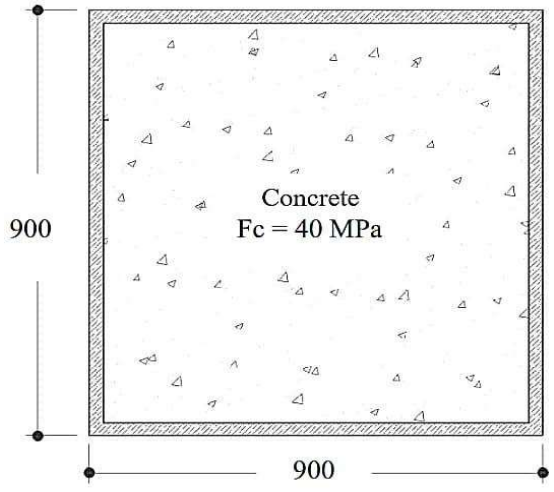

Figure 4. *Column cross-section*

Based on ***Table 1****, the dimensions of the columns and beams vary every 10 floors. This will certainly provide an overview of the behavior and structural mass of each model.*

Table 1. *Profile used*

System	Profile Placement	Structural Profile Uesd	
		Column (CFST)	Beam (WF)
MRF	Floor 1-10	1000x1000x19	600x300x12x20
MRF	Floor 11-20	900 x 900 x 19	600x300x12x17
MRF	Floor 21-30	900 x 900 x 16	600x200x13x23
CBF	Floor 1-10	900 x 900 x 12	600x200x12x20
CBF	Floor 11-20	800 x 800 x 12	600x200x11x17
CBF	Floor 21-30	700 x 700 x 12	600x200x10x15

The CFST columns used are a combination of unreinforced concrete encased in a steel plate. ***Figure 4*** *shows one of the column cross-section dimensions, which is 900x900x12.*

The use of lighter profiles on the upper floors aims to optimize the structural mass. On the higher levels, the gravity loads supported by the columns are significantly lower than those at the base. Consequently, by reducing the profile sizes, the total weight of the building is significantly decreased.

Profile changes can be utilized to regulate the natural period of the building. In RSA (Response Spectrum Analysis), these adjustments ensure the structure is not excessively stiff while still satisfying drift requirements. A controlled reduction of stiffness in the upper floors helps distribute seismic energy dissipation more evenly across the entire height of the building.

The following technical parameters are employed:

Steel grade = BJ 41
fy = 250 MPa
fu = 410 MPa
Concrete grade = 40 MPa
Slab thickness = 120 mm
Longitudinal reinforcement = D21
Distribution reinforcement = D13
Bracing profile = WF 300.300.11.17
Secondary beam profile
Roof beam (span 8m) = WF 350.175.6.9
Roof beam (span 6m) = WF 250.175.7.11
Floor beam (span 8m) = WF 350.250.8.12
Floor beam (span 6m) = WF 250.175.7.11

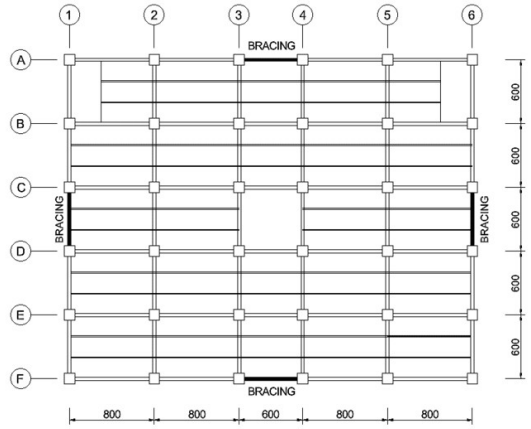

Figure 5. *Floor plan*

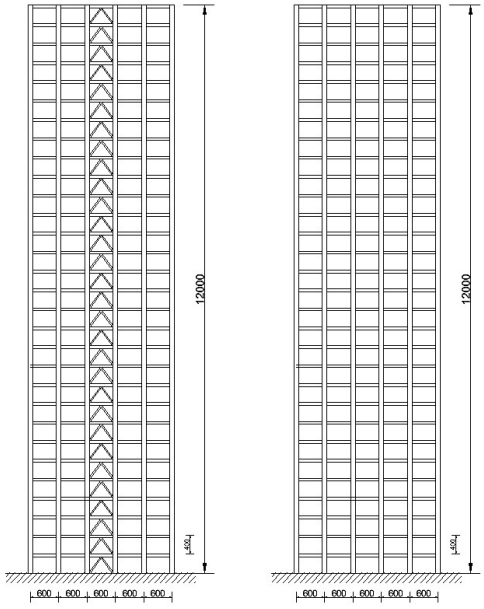

(a) *(b)*

Figure 6. *Cross section of building (a) CBF and (b) MRF*

In civil engineering, structural loading is the process of determining all forces that will act on a building. This is a fundamental step to ensure that every structural element is capable of safely resisting these forces.

a. Dead Load

The self-weight (dead load) of building elements is calculated by multiplying the unit weight of the material by the volume of the element. The unit weight of steel is 7850 kg/m³, while that of concrete is 2400 kg/m³. The calculation of self-weight can also be performed automatically using structural analysis software once the modeling process is completed.

b. Superimposed Dead Load

The superimposed dead loads are determined based on SNI 1727:2020[18]. The applied loads are shown in ***Table 2****.*

Table 2. *Load data*

Building Components	*Weight (kN/m³)*	*Quantity (m)*	*Load (kN/m²)*
Load on the slab (distributed load)			
Sand (10 mm)	*16*	*0.01*	*0.16*
Mortar (30 mm)	*21*	*0.03*	*0.63*
Ceramic Tile (20 mm)	*24*	*0.02*	*0.48*
Acoustic Ceiling + Hanger System	*0.20*		*0.20*
Partition Wall	*0.57*		*0.57*
MEP Installation	*0.25*		*0.25*
Total			*2,29*
Load on the beam (line load)			
Lightweight brick wall	*3.06*	*6*	*2.754*
construction	*3.06*	*8*	*3.672*

c. Live Load

The live load for office building is taken as 2.40 kN/m² uniformly distributed from 1st to the 29th floor in accordance with Table 4.3-1 SNI 1727-2020 [18] and for corridor load is 2.50 kN/m². Meanwhile for the roof live load, a value of 0.96 kN/m2 is applied.

d. Earthquake Load

Risk Category = II
Seismic Importance Factor (Ie) = 1.00
Soil Classification = SC (hard soil, dense soil, and soft rock)

Table 3. *N-SPT*

No.	*Soil Type, Penetration, NSPT*	*Boring*
1	*Clayey soil, yellowish brown*	*0.00-0.75*
	Thickness (m)	*3*
	N-SPT	*30*
2	*Clayshale, light grey*	*4.68-5.00*
	Thickness (m)	*6*
	N-SPT	*40*
3	*Claystone, light grey*	*9.14-9.77*
	Thickness (m)	*2*
	N-SPT	*60*
4	*Claystone, dark grey*	*10.00-11.55*
	Thickness (m)	*3*
	N-SPT	*60*
5	*Claystone, dark grey*	*14.40-15.00*
	Thickness (m)	*7*
	N-SPT	*60*
6	*Clayshale, dark grey*	*23.10-23.70*
	Thickness (m)	*6*
	N-SPT	*60*
7	*Claystone, dark grey*	*29.00-29.65*
	Thickness (m)	*3*
	N-SPT	*60*

*The calculation for determining soil classification is based on the N-SPT test data presented in **Table 3**. Computed using the following **Equation 1**:*

$$\bar{N} = \frac{\sum_{i-1}^{n} d_i}{\sum_{i-1}^{n} \frac{d_i}{N_i}} \quad (1)$$

$$\sum_{i-1}^{n} d_i = 370$$

$$\sum_{i-1}^{n} \frac{d_i}{N_i} = 1.652$$

$$\bar{N} = \frac{\sum_{i-1}^{n} d_i}{\sum_{i-1}^{n} \frac{d_i}{N_i}} = \frac{370}{1.652} = 223.971$$

Based on those calculations, the soil classification is categorized as Site Class SC (hard soil, very dense soil, and soft rock) in accordance with the parameters set forth in SNI 1726:2019 Ps. 5.3 Table 5.

This study employs the Elastic Response Spectrum Analysis (RSA) method as the primary instrument for evaluating the seismic performance of the structural system. This method was selected for its capability to represent comprehensive dynamic structural behavior through the combination of various natural vibration modes contributing to the total response of the building. The analysis is conducted by mapping seismic accelerations from the design response spectrum—referencing the RSA Cipta Karya parameters for the IKN region—into a linear-elastic mathematical model of the structure. RSA method generates estimates for base shear, internal forces, and story drift, which are essential to ensure that the high-rise building design remains within the safety limits mandated by applicable seismic standards.

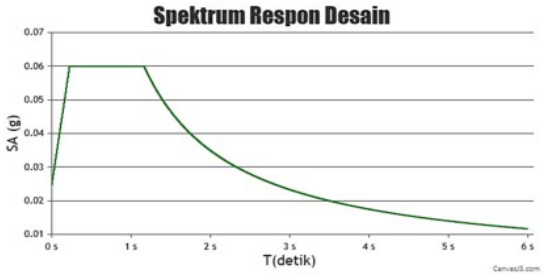

***Figure 7.** Design respon spetrum (Source: RSA Cipta Karya)*

***Figure 8.** Design spectrum parameters (Source: RSA Cipta Karya)*

Design Spectrum Parameter that shown based on Figure 8 consist of:

T0 (second)	*= 0.23 second*
Ts (second)	*= 1.17 second*
Sds (g)	*= 0.06 g*
Sd1 (g)	*= 0.07 g*
PGA MCEG	*= 0.0421 g*
SS MCEr	*= 0.0688 g*
S1 MCEr	*= 0.0754 g*

***Table 4.** Falue of Fa*

Site Calss	*The risk-targeted maximum considered earthquake (MCE_R) spectral response acceleration parameter mapped at the short-period, T = 0,2 seconds, S_s*					
	$S_s \leq 0{,}25$	$S_s = 0{,}5$	$S_s = 0{,}75$	$S_s = 1{,}0$	$S_s = 1{,}25$	$S_s \geq 0{,}25$
SA	*0.8*	*0.8*	*0.8*	*0.8*	*0.8*	*0.8*
SB	*0.9*	*0.9*	*0.9*	*0.9*	*0.9*	*0.9*
SC	*1.3*	*1.3*	*1.2*	*1.2*	*1.2*	*1.2*
SD	*1.6*	*1.4*	*1.2*	*1.1*	*1.0*	*1.0*
SE	*2.4*	*1.7*	*1.3*	*1.1*	*0.9*	*0.8*
SF	$SS^{(a)}$					

Source: Table 6 of SNI 1726:2019 [19]

*Based on the soil classification according to **Table 4**, the value of Fa (short-period amplification factor) is 1.3.*

***Table 5.** Falue of Fv*

Site Calss	*The risk-targeted maximum considered earthquake (MCE_R) spectral response acceleration parameter mapped at the short-period, T = 1 second, S_s*					
	$S_s \leq 0{,}1$	$S_s = 0{,}2$	$S_s = 0{,}3$	$S_s = 0{,}4$	$S_s = 0{,}5$	$S_s \geq 0{,}6$
SA	*0.8*	*0.8*	*0.8*	*0.8*	*0.8*	*0.8*
SB	*0.8*	*0.8*	*0.8*	*0.8*	*0.8*	*0.8*
SC	*1.5*	*1.5*	*1.5*	*1.5*	*1.5*	*1.4*
SD	*2.4*	*2.2*	*2.0*	*1.9*	*1.8*	*1.7*
SE	*4.2*	*3.3*	*2.8*	*2.4*	*2.2*	*2.0*
SF	$SS^{(a)}$					

Source: Table 6 of SNI 1726:2019 [19]

*Based on the soil classification according to **Table 5**, the value of Fv (long-period amplification factor) is 1.5.*

3. Result and Discussion

*The 3D modeling of the 30-story building structure, as shown in **Figure 8**, is a complex and crucial process in modern civil engineering. It involves creating an accurate virtual model of the entire building framework, including elements such as columns, beams, slabs, and bracing. The purpose is to analyze the structural behavior under various loading conditions, ensuring safety, efficiency, and compliance with applicable design standards. **Figure 9** presents the 3D structural model and the cross section with*

concentric braced frames as the lateral system, while ***Figure 10*** *shows the 3D structural model and the cross section with a moment-resisting frame system.*

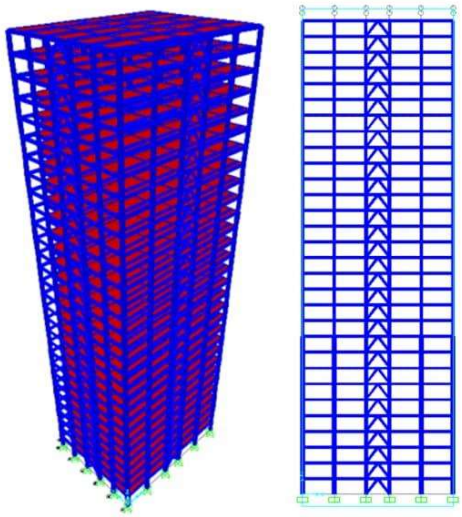

Figure 9. *Models of CBF system (a) 3D and (b) Cross section*

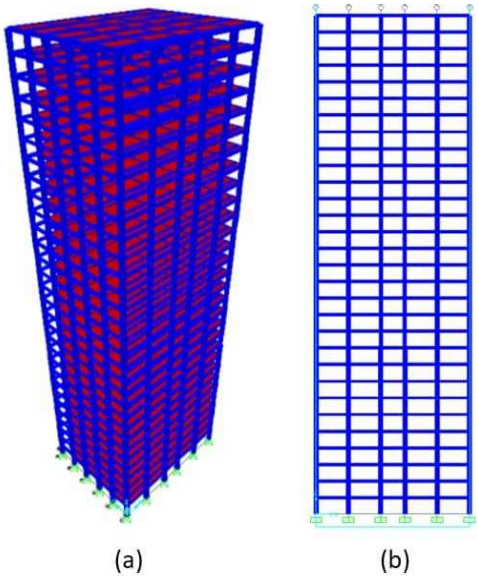

Figure 10. *Models of MRF system (a) 3D and (b) Cross section*

Before a structural design is approved for construction, every element must undergo a rigorous structural analysis control process. This process ensures that the structure is capable of carrying the intended loads and remains stable under all conditions. According to the seismic code SNI, Ps. 7.9.1, the analysis must include a sufficient number of modes to achieve a combined modal mass participation of at least 90% of the actual modeled mass.

Modal Load Participation Ratios

File View Edit Format-Filter-Sort Select Options

Units: As Noted
Filter:

	OutputCase	ItemType Text	Item Text	Static Percent	Dynamic Percent
▶	MODAL	Acceleration	UX	99,9865	94,8134
	MODAL	Acceleration	UY	99,9725	93,6685
	MODAL	Acceleration	UZ	0,0076	0,0001953

(a)

Modal Load Participation Ratios

File View Edit Format-Filter-Sort Select Options

Units: As Noted
Filter:

	OutputCase	ItemType Text	Item Text	Static Percent	Dynamic Percent
▶	MODAL	Acceleration	UX	99,9704	92,7747
	MODAL	Acceleration	UY	99,9702	92,9758
	MODAL	Acceleration	UZ	0,0038	8,507E-05

(b)

Figure 11. *Output of modal mass participation ratio for (a) CBF and (b) MRF models*

The modal mass participation ratios in both models show values exceeding 90%, indicating that the structural analysis has satisfied the requirements specified in SNI 1726:2020, Ps. 7.9.1. Subsequently, a comparison of the structural mass is carried out to evaluate the effectiveness of mass in relation to the influence of seismic forces.

Base Reactions

File View Edit Format-Filter-Sort Select Options

Units: As Noted
Filter:

	OutputCase	CaseType Text	GlobalFX KN	GlobalFY KN	GlobalFZ KN
▶	1D+1L	Combination	2,81E-10	-8,035E-10	348920,632

(a)

Base Reactions

File View Edit Format-Filter-Sort Select Options

Units: As Noted
Filter:

	OutputCase	CaseType Text	GlobalFX KN	GlobalFY KN	GlobalFZ KN
▶	1D+1L	Combination	1,969E-10	7,514E-11	372651,354

(b)

Figure 12. *Output mass structure (a) CBF and (b) MRF models*

The structural mass values of both models were obtained from the output of the structural analysis software. Based on the analysis results, the structural mass of the CBF model is

348920.632 kN, while the structural mass of the MRF model is 372651.354 kN.

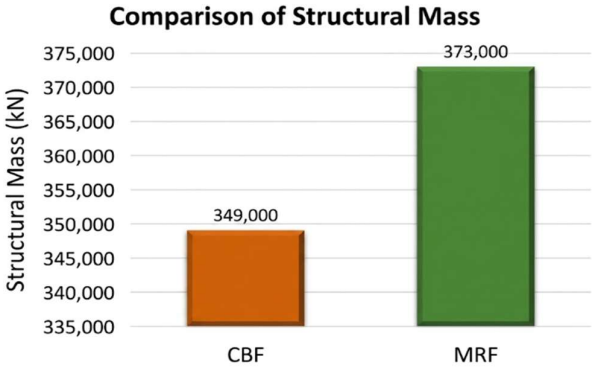

Figure 13. *Structure mass comparison graph*

When presented in graphical form, as shown in ***Figure 13****, the differences in structural mass between the two models become evident. The structural mass of the MRF model is significantly larger than that of the CBF model, with a difference of 23730,722 kN or equivalent to 6,8%.*

The greater the building mass, the larger the inertia force or effective seismic force acting on the structure. Conversely, a lighter structure produces smaller inertia forces during an earthquake. This means that a lighter building mass reduces the loads that must be resisted by structural elements such as columns and beams. Based on the comparison of structural masses, the CBF system is more effective in resisting seismic forces, whereas the MRF model has the potential to cause more severe damage if not properly designed.

Table 6. *Shear force*

Model	*Base Shear*	*Static Base Shear (kN)*	*Dynamic Base Shear (kN)*	*0,85. Static Base Shear*	*Scale Factor* $(0.85\ V_{static} / V_{dynamic})$	*Control* $V_d > 85\%.V_s$
CBF	*X*	*685.877*	*2946.197*	*2504.2675*	*3.651*	*OK*
CBF	*Y*	*755.881*	*2946.197*	*2504.2675*	*3.313*	*OK*
MRF	*X*	*510.477*	*3180.183*	*2703.1556*	*5.295*	*OK*
MRF	*Y*	*579.131*	*3180.183*	*2703.1556*	*4.668*	*OK*

For the comparison of base shear forces, according to the seismic code SNI 1726:2019 Ps. 7.9.4.1 on force scaling, the regulation stipulates that the dynamic base shear must be greater than 85% of the static base shear, expressed as VD > 85% VS. If this requirement is not satisfied, a force scaling factor must be applied to the building model.

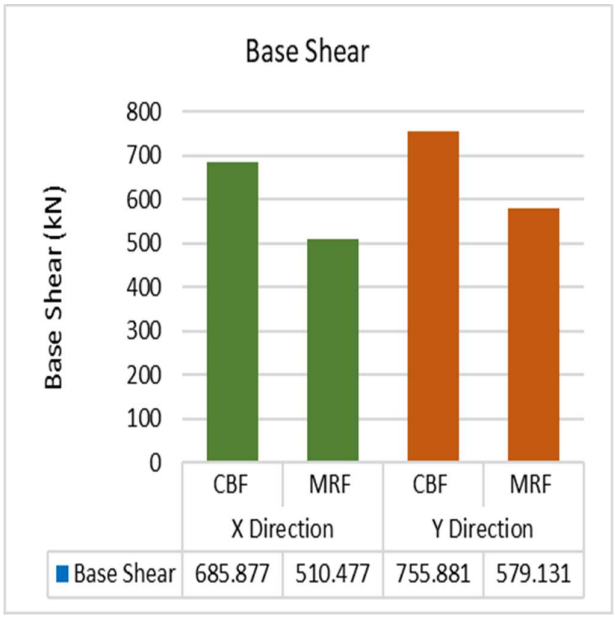

Figure 14. *Comparison graph of base shear*

From ***Table 6*** *and* ***Figure 14****, it can be observed that the value of the static base shear (Vstatic) in the CBF model is greater than that in the MRF model. This is due to its more limited capability to dissipate energy through inelastic deformation, requiring the structure to be designed with greater strength in order to withstand higher seismic forces elastically. However, in principle, the analysis results of the base shear for both the CBF and MRF models have satisfied the standards specified in SNI 1726:2019.*

Subsequently, a comparative analysis of displacement and story drift is carried out for the structure in both the X and Y directions. The inter-story drift is defined as the difference between the amplified elastic displacement at a given story and the amplified elastic displacement at the story below. This drift value is then checked against the drift limit of 0.02 hsx. The deflection of the center of mass at story x (δx) must be determined according to the following ***Equation 2****:*

$$\delta_x = \frac{C_d \cdot \delta_{xe}}{I_e} \quad \textit{(SNI 1726:2019 Eq. 67 Ps. 7.12.3)} \quad (2)$$

Where

Cd = Deflection amplification factor (5.5)

δxe = Deflection at story x as determined from elastic analysis.

Ie = Importance Factor (1.0).

Δa = 0,020hsx (allowable story drift limit

ρ = Redundancy factor (1.0)

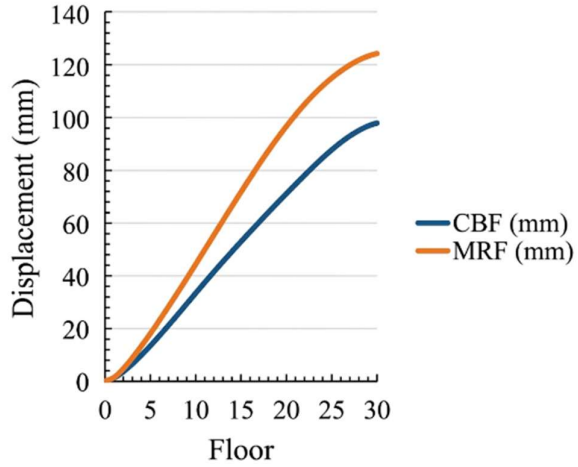

Figure 15. *Comparison graph of displacement in the X-direction*

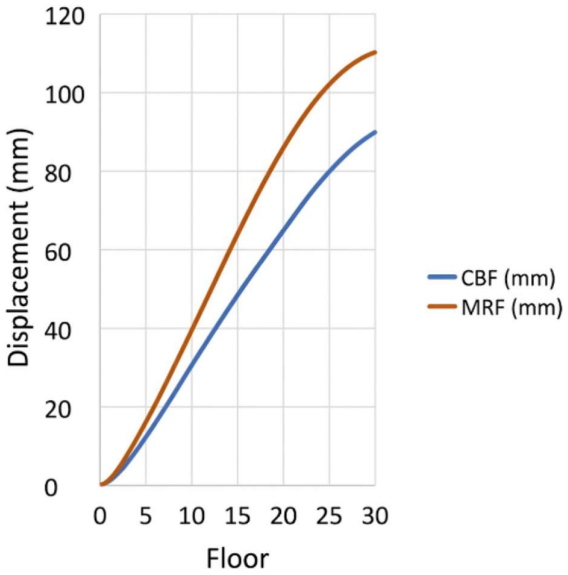

Figure 16. *Comparison graph of displacement in the Y-direction*

Figure 15 *and* ***Figure 16*** *visually demonstrate that for a 30-story building, in both the X and Y directions, the concentric braced frame (CBF) system is stiffer than the moment-resisting frame (MRF) system. The total lateral displacement at each story for the CBF system is consistently smaller than that of the MRF system. This difference becomes more significant as the building height increases. This confirms the theoretical characteristics of the two structural systems, where the CBF system is more effective in limiting lateral displacement, while the MRF system, although offering greater architectural flexibility, results in larger drift.*

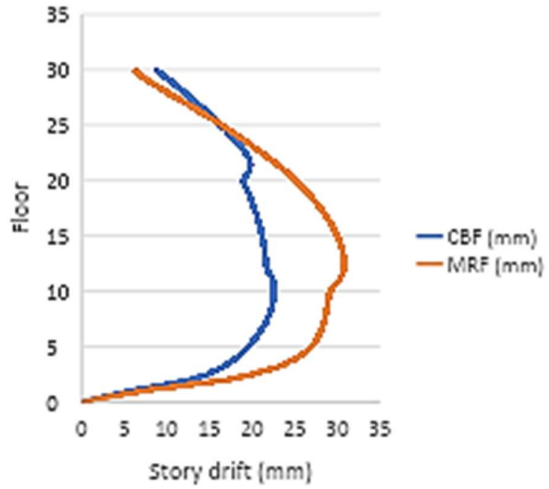

Figure 17. *Graph of story drift comparison in X-direction*

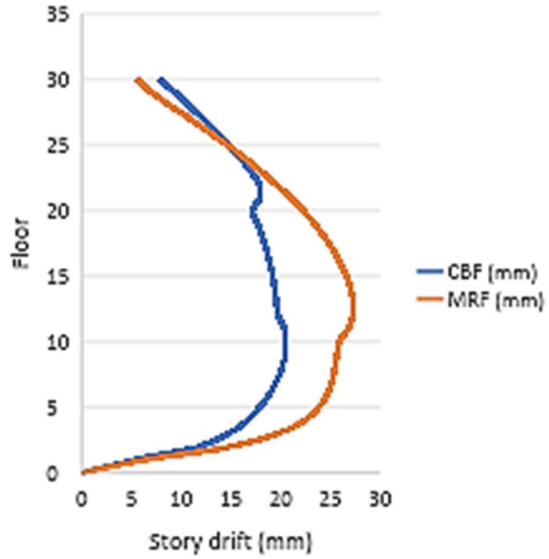

Gambar 18. *Graph of story drift comparison in Y-direction*

Based on the comparison graph of story drift in the X and Y directions, it can be seen from ***Figure 17*** *and* ***Figure 18*** *that the inter-story drift values still meet the requirements, as the values are less than 80 mm in accordance with SNI 1726:2019 Ps. 7.12.1 Table 20. This is strongly influenced by the use of CFST columns, which help reduce drift values and make the structure stiffer.*

In terms of drift patterns, different behaviors are observed. The curve for the MRF system (orange line) shows significantly larger inter-story drift in the middle part of the building (around floors 10–15) compared to the CBF system

(blue line). The MRF system experiences maximum inter-story drift (30.791 mm) at floors 10 to 15, while the CBF system experiences a smaller maximum drift is 22.544 mm. The more pronounced curve of the MRF system in the middle portion indicates that this system has relatively lower stiffness in that area, leading to greater deformation. On the other hand, the gentler slope and lower peak of the CBF curve demonstrate that the system is overall stiffer and more effective in limiting inter-story drift.

The displacement values in the CBF system are significantly lower than those of the MRF system due to fundamental differences in lateral force transfer mechanisms. In an MRF system, lateral loads are resisted through the bending action of beams and columns as well as rotation at rigid joints, which inherently results in larger deformations due to the limitations of flexural stiffness. Conversely, the CBF system utilizes diagonal elements to form a truss system that transfers lateral loads into axial tension and compression forces. Given that steel exhibits much higher stiffness efficiency in resisting axial loads compared to flexural loads, the presence of these braces provides a drastic stiffening effect, thereby more dominantly limiting structural sway.

This phenomenon is consistent with structural theory, which states that CBF effectively increases the effective lateral stiffness of a building, providing superior stability compared to MRF, which relies heavily on the strength of moment connections. The integration of CFST columns within the CBF system further reinforces this behavior, as the infill concrete provides support against local buckling of the steel profiles, while the bracing ensures the structure remains within a small deformation range. With higher stiffness, this system not only satisfies story drift requirements more easily but is also effective in mitigating P-Delta effects, which are often a major constraint on the stability of high-rise structures in seismically active regions like IKN.

4. Conclusion

Based on the research conducted on a 30-story building structure using the CBF and MRF systems with predetermined dimensions, structural modeling was carried out using structural analysis software by applying two systems, namely CBF (Concentrically Braced Frame) and MRF (Moment Resisting Frame). A design check was performed to ensure that the modeling in the software complies with the requirements and criteria set by the applicable regulations. For the mass participation ratio check, both models satisfied the requirement, showing values above 90% in accordance with SNI 1726:2020 Ps. 7.9.1. The structural mass of the CBF model was 348,920.632 kN, while the MRF model had a structural mass of 372,651.354 kN. The mass difference between the two systems is 23,730 kN, or 6.8%. The lighter structural mass of the CBF model indicates that it has better performance compared to the MRF model in resisting seismic forces when evaluated in terms of structural mass comparison. For the base shear check, both CBF and MRF models met the requirements specified in SNI 1726:2019 Ps 7.9.4.1, with dynamic shear force factors satisfying Vdynamic > 85% Vstatic. Meanwhile, for displacement control in both X and Y directions, the total lateral displacement at each story in the CBF system consistently showed smaller values compared to the MRF system. The maximum displacement of CBF is 98.496 mm, and for MRF is 123.972 mm. This indicates that the implementation of the bracing system in the CBF successfully reduces displacement by 25.476 mm, or approximately 20.55%, compared to the MRF system. This significant reduction proves that the CBF system provides higher lateral stiffness, which is crucial for limiting structural deformation in high-rise buildings within the IKN region.In the analysis of story drift in both X and Y directions, the results also met the requirement, where the values must remain below 80 mm. This condition is also influenced by the use of CFST columns, which help reduce drift and increase structural stiffness. However, based on the comparison graphs, different drift patterns were observed: the MRF system exhibited significantly larger story drift compared to the CBF system, indicating relatively lower stiffness and therefore larger deformation.

References

[1] R. Sabelli, C. W. Roeder, and J. F. Hajjar, "Seismic Design of Steel Special Concentrically Braced Frame Systems A Guide for Practicing Engineers," no. 8, pp. 1–36, 2013.

[2] A. Giroth, B. D. Handono, and S. O. Dapas, "Perencanaan Struktur Gedung Bertingkat Tahan Gempa Menggunakan Sistem Rangka Baja Terbreis Konsentris Khusus (Studi Kasus: Rumah Sakit Di Kota Manado)," Tahun, vol. 22, no. 88, p. p-ISSN, 2024.

[3] M. Aldaw, M. A. Ahmed Aldaw, and A. Suryadi, "Comparison Between Concentric Bracing Frame and Eccentric Bracing Frame in Earthquake-Resistant High-Rise Buildings," vol. 4, no. 3, pp. 111–116, 2023, [Online]. Available: https://www.researchgate.net/publication/380753083

[4] *R. K.P. and M. S. George, "Disposable Knee Bracing in Combined Bracing System-Improvement in Seismic Design of Steel Frame using ETABS," vol. 10, no. 06, pp. 170–179, 2022, [Online]. Available: www.ijert.org*

[5] *N. Goswami, "A Review on the Analysis of Building with Different Types of Bracings," Int J Res Appl Sci Eng Technol, vol. 10, no. 3, pp. 215–218, 2022, doi: 10.22214/ijraset.2022.40556.*

[6] *A. Kanyilmaz, "Secondary frame action in concentrically braced frames designed for moderate seismicity: a full scale experimental study," Bulletin of Earthquake Engineering, vol. 15, 2017, doi: 10.1007/s10518-016-0054-x.*

[7] *M. Mahdavi, "Evaluating the Seismic Performance of Modern Concentrically Braces with the Finite Element Method," Advance Researches in Civil Engineering, vol. 5, no. 3, pp. 68–76, 2023, doi: 10.30469/ARCE.2024.449526.1070.*

[8] *A. Janbandhu, P. Singh, K. R. Dabhekar, I. Khedikar, and J. V. Shukla, "Effect of Various Concentric Bracing in Building," IOP Conf Ser Earth Environ Sci, vol. 1193, no. 1, 2023, doi: 10.1088/1755-1315/1193/1/012014.*

[9] *Y. S. Yoganata, "Analisis Pengaruh Penggunaan Bresing Pada Struktur Bangunan Baja 20 Lantai," 2023, JOS MRK, Malang.*

[10] *P. Roshan, R. K. Meena, and I. Singh, "Analyzing the Effectiveness of Bracing Patterns in High-Rise Building," Advances in Transdisciplinary Engineering, vol. 43, pp. 144–150, 2023, doi: 10.3233/ATDE230712.*

[11] *H.-W. Gu et al., "Experimental study on seismic performance of CFST columns under ambient temperature effects," ScienceDirect, vol. 493, no. Construction and Building Materials, 2025, doi: https://doi.org/10.1016/j.conbuildmat.2025.143018.*

[12] *H. Chen, L. Wu, H. Jiang, and Y. Liu, "Seismic performance of prefabricated middle frame composed of special-shaped columns with built-in lattice concrete-filled circular steel pipes," Elsevier Structure, vol. 34, pp. 1443–1457, 2021, doi: https://doi.org/10.1016/j.istruc.2021.08.062.*

[13] *J. Y. R. Liew, M. Xiong, and D. Xiong, "Design of Concrete Filled Tubular Beam-columns with High Strength Steel and Concrete," ScienceDirect, vol. 8 Part. 2, no. Structures, pp. 213–226, 2016, doi: https://doi.org/10.1016/j.istruc.2016.05.005.*

[14] *Y. Zheng, Z. Lin, Y. Lin, and X. Zhang, "Eccentric compressive behavior of stiffened and multi-cell cross-shaped CFST columns under different loading angles," ScienceDirect, no. Thin-Walled Structures, 2025, doi: https://doi.org/10.1016/j.tws.2025.113903.*

[15] *X. Li, S. Zhang, B. Song, and Z. Huang, "Eccentric compression behavior of CFST columns strengthened with steel tube and sandwiched grout jackets," ScienceDirect, vol. 215, 2025, doi: https://doi.org/10.1016/j.tws.2025.113565.*

[16] *H. Huang, L. Guo, J. Chen, J. Li, and Z. Wang, "Axial compressive behavior of circular CFST stub columns with pitting corrosion," J Constr Steel Res, vol. 235, p. 109809, Dec. 2025, doi: 10.1016/J.JCSR.2025.109809.*

[17] *B. Zhang, "Challenges in the Application of Concentric Bracing for Tall Buildings: Structural Considerations," Eng Struct, p. 257, 2023.*

[18] *Badan Standardisasi Nasional, "Beban desain minimum dan Kriteria terkait untuk bangunan gedung dan struktur lain 1727:2020," Badan Standarisasi Nasional 1727:2020, no. 8, pp. 1–336, 2020.*

[19] *Badan Standarisasi Nasional, "SNI-1726-2019-Tata cara perencanaan ketahanan gempa untuk bangunan gedung dan nongedung," vol. 1726:2019, pp. 1–254, 2019.*